CHEMISTRY OF MATERIALS

Article

pubs.acs.org/cm

Advancing Biocapture Substrates via Chemical Lift-Off Lithography

Huan H. Cao,[†,‡] Nako Nakatsuka,[†,‡] Wei-Ssu Liao,[†,‡] Andrew C. Serino,[†,‡,§] Sarawut Cheunkar,[†,‡] Hongyan Yang,[∥] Paul S. Weiss,*[,†,‡,§] and Anne M. Andrews*[,†,‡,∥]

[†]California NanoSystems Institute, University of California, Los Angeles, California 90095, United States

[‡]Department of Chemistry and Biochemistry, University of California, Los Angeles, California 90095, United States

[§]Department of Materials Science and Engineering, University of California, Los Angeles, California 90095, United States

[∥]Department of Psychiatry and Biobehavioral Sciences, Semel Institute for Neuroscience and Human Behavior, and Hatos Center for Neuropharmacology, University of California, Los Angeles, California 90095, United States

Supporting Information

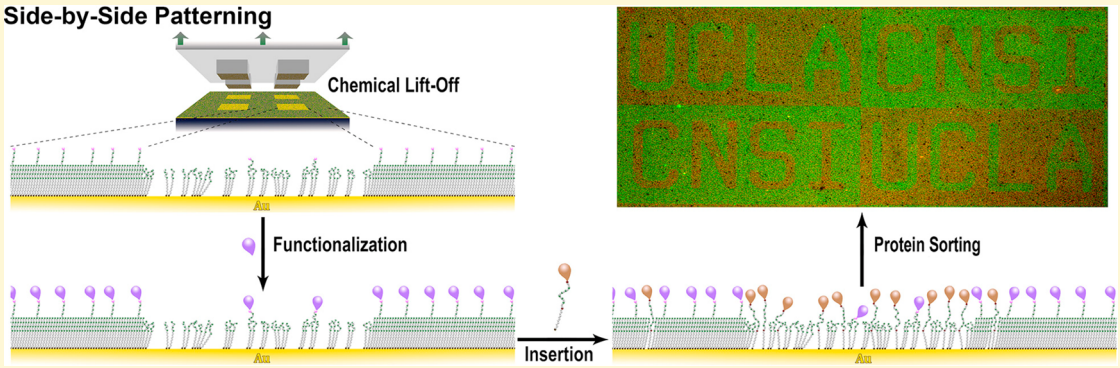

ABSTRACT: Creating small-molecule-functionalized platforms for high-throughput screening or biosensing applications requires precise placement of probes on solid substrates and the ability to capture and to sort targets from multicomponent samples. Here, chemical lift-off lithography was used to fabricate large-area, high-fidelity patterns of small-molecule probes. Lift-off lithography enables biotin−streptavidin patterned recognition with feature sizes ranging from micrometers to below 30 nm. Subtractive patterning via lift-off facilitated insertion of a different type of molecule and, thus, multiplexed side-by-side placement of small-molecule probes such that binding partners were directed to cognate probes from solution. Small molecules mimicking endogenous neurotransmitters were patterned using lift-off lithography to capture native membrane-associated receptors. We characterized patterning of alkanethiols that self-assemble on Au having different terminal functional groups to expand the library of molecules amenable to lift-off lithography enabling a wide range of functionalization chemistries for use with this simple and versatile patterning method.

■ INTRODUCTION

To produce multiplexed, functional, biocapture platforms for high-throughput screening or biosensing applications, surface patterning and immobilization strategies are needed to anchor molecules on solid substrates for capturing and sorting respective binding partners from complex mixtures in solution or *in vivo*.[1−11] Although *in vivo* sensing to date has been based largely on electrochemical[12−14] or enzymatic detection,[15−17] small-molecule biocapture strategies provide gateways to new sensing opportunities.[18] Immobilization of large biomolecules on surfaces requires avoiding denaturation upon surface adsorption and favorable orientation for ligand binding.[19−24] In contrast, surface tethering of small-molecule probes necessitates judicious selection of coupling chemistries and surface dilution to facilitate recognition by large biomolecule binding partners.[22,25−32] For instance, the areal size mismatch on surfaces between small-molecule neurotransmitters or amino acids and large antibody or receptor binding partners is >100-fold.[33,34]

An important goal of small-molecule chemical patterning is site-specific placement of multiple probes on substrates for the interrogation of target binding specificity and selectivity.[32,35−38] However, achieving this objective has been challenging.[39−43] We developed additive methods to pattern small molecules to investigate biomolecule capture via relative quantification of binding on functionalized versus unfunctionalized regions of substrates. Microcontact insertion printing (μCIP) was used to pattern small-molecule neurotransmitters and precursors mimicking endogenous neurotransmitters on alkanethiol self-assembled monolayer (SAM)-modified Au substrates.[44−46] Using this approach, molecular tethers are inserted into

Received: May 12, 2017
Revised: July 18, 2017
Published: July 24, 2017

DOI: 10.1021/acs.chemmater.7b01970
Chem. Mater. XXXX, XXX, XXX−XXX

preformed SAMs, and tethers are functionalized on-substrate with small-molecule probes. To circumvent problems associated with the sequential surface functionalization chemistries needed for multifunctionalized substrates, we used microfluidics to generate multiplexed substrates.[38] Here, two-component SAMs with low proportions of tether molecules (<10% solution concentration) are produced by codeposition to achieve dilution of surface tethers. Individual channels are exposed to different small-molecule targets for multiplexed functionalization.

We also developed a subtractive patterning method called chemical lift-off lithography, where alkanethiol SAM molecules are removed from Au substrates.[47,48] Polydimethylsiloxane (PDMS) stamps are treated with oxygen plasma to generate siloxyl groups on stamp surfaces. Activated stamps are brought into conformal contact with hydroxyl-terminated alkanethiol SAMs (or other suitably terminated monolayers) on Au substrates to produce covalent interactions at stamp/SAM interfaces. Previous studies indicated the lability of Au−Au bonds at substrate−SAM interfaces based on evidence for mobile Au thiolates within SAMs[49−52] and the presence of low-coordination Au adatoms beneath SAMs.[53−55] Zhang et al. used thiol-derivatized tips and atomic force microscopy (AFM) to quantify the strengths of isolated Au−S bonds.[56] They showed that Au−S bonds were sufficiently strong such that Au−Au bonds at the outermost Au-substrate layers can be preferentially disrupted. We have shown that stamp/SAM and SAM/Au interfacial interactions in lift-off lithography are stronger than Au−Au substrate bonds as stamp lift-off causes alkanethiols and the outermost layer of the underlying Au atoms to be simultaneously removed.[47]

Previously, lift-off regions were patterned with biotin-terminated alkanethiols to capture streptavidin.[47] Lift-off removes a significant portion of the initial monolayer. Yet, molecules remaining in the contact regions facilitate controlled and favorable insertion of new molecules. For example, DNA probes can be inserted into lift-off regions for highly efficient and tunable hybridization with complementary oligomers.[57] Chemical lift-off lithography has also been combined with sol−gel chemistry to print transistors for small-molecule biosensors.[58]

Here, we advance the understanding, use, and applicability of chemical lift-off lithography. We expand the feature shapes and sizes patterned by lift-off lithography and extend nanoscale patterning by this method to sub-30 nm using a single lift-off step. We produce bifunctional substrates to demonstrate biomolecule recognition and sorting. We use lift-off lithography to produce patterned substrates that capture native protein targets. In addition, alkanethiols with a range of terminal functionalities are investigated to enlarge the molecular library that can be patterned by chemical lift-off lithography.

■ EXPERIMENTAL SECTION

Materials. Silicon substrates with 100 nm Au films over 10 nm Ti adhesive layers were purchased from Platypus Technologies (Madison, WI). 6-Mercaptohexanol (MCH), 1-dodecanethiol (CH_3−C11), *N*-hydroxysuccinimide (NHS), *N*-(3-(dimethylamino)propyl)-*N*′-ethylcarbodiimide hydrochloride (EDC), *N*,*N*-dimethylformamide (DMF), 4-methylpiperidine, bovine serum albumin (BSA), and 0.01 M phosphate buffered saline (PBS) ([NaCl] = 138 mM, [KCl] = 2.7 mM pH 7.4) were purchased from Sigma-Aldrich (St. Louis, MO). Absolute, 200 proof, anhydrous, ACS/USP grade ethyl alcohol was from PHARMCO-AAPER (Oakland, CA). Deionized water (∼18 MΩ) was obtained from a Millipore water purifier (Billerica, MA). The FMOC-protected biological precursors to serotonin and dopamine, i.e., 9-fluorenylmethyloxycarbonyl-5-hydroxy-L-tryptophan (FMOC-L-5HTP) and 9-fluorenylmethyloxycarbonyl-3,4-dihydroxy-L-phenylalanine (FMOC-L-DOPA), were purchased from AnaSpec-Eurogentec (Fremont, CA).

(11-Mercaptoundecyl)tri(ethylene glycol) (TEG) and (11-mercaptoundecyl)hexa(ethylene glycol)carboxylic acid (COOH-HEG) were purchased from Toronto Research Chemicals Inc. (Toronto, ON, Canada). 11-Mercaptoundecyl hexa(ethylene glycol)-biotin (biotinylated hexa(ethylene glycol)undecanethiol; BEG) was from Nanoscience Instruments Inc. (Phoenix, AZ). 11-Bromo-1-undecanethiol (Br-C11) was obtained from Assemblon Inc. (Redmond, WA). (11-Mercaptoundecyl)hexa(ethylene glycol)amine (AEG), 11-mercaptoundecylphosphonic acid ($PO(OH)_2$-C11), and (11-mercaptoundecyl)tri(ethylene glycol)methyl ether (CH_3O-TEG) were from Prochimia (Sopot, Poland).

Streptavidin antibodies (1 mg/mL) and AlexaFluor 546 goat antimouse IgG (H+L) highly cross-adsorbed antibodies (2 mg/mL) were purchased from Invitrogen (Carlsbad, CA). Mouse polyclonal antiserotonin$_{1A}$ (5-HT_{1A}) receptor antibodies (whole antiserum), rabbit polyclonal antidopamine D_1 receptor antibodies (whole antiserum), mouse monoclonal anti-L-5-HTP antibodies (1 mg/mL), mouse monoclonal anti-L-DOPA antibodies (1 mg/mL), and fluorescein isothiocyanate (FITC)-conjugated rabbit polyclonal antistreptavidin antibodies (10 mg/mL) were purchased from Abcam Inc. (Cambridge, MA). Human 5-HT_{1A} receptors (0.8 fmol receptor protein/μg membrane protein; 6.4 μg/μL total protein concentration) from transfected human embryonic kidney 293 (HEK293) cells and untransfected HEK293 cell membranes (10 μg/μL total protein concentration) were from PerkinElmer, Inc. (Waltham, MA). All antibodies and proteins were used as received and incubated with substrates in 0.01 M PBS pH 7.4 at room temperature. Antibodies not labeled with fluorophores and fluorescently labeled antibodies were diluted 1:200 and 1:100, respectively, in 0.01 M PBS pH 7.4.

Substrate and Stamp Preparation. All Au substrates were hydrogen-flame annealed, followed by incubation with ethanolic solutions of alkanethiols. After monolayer formation, substrates were rinsed thoroughly with fresh ethanol and dried with nitrogen gas. Different feature shapes on polydimethylsiloxane (PDMS) stamps were produced from silicon masters, which were fabricated by standard photolithography. The process of stamp fabrication and details of oxygen plasma treatment are published elsewhere.[38,46,47,57]

Briefly, a 10:1 mass ratio of SYLGARD 184 silicone elastomer base and curing agent (Ellsworth Adhesives, Germantown, WI) was mixed thoroughly in a plastic cup, degassed under vacuum, cast onto master substrates in plastic Petri dishes, and cured in an oven at 70 °C overnight. Polymerized stamps were removed from masters, cut into usable sizes, and treated with oxygen plasma (Harrick Plasma, power 18 W, and oxygen pressure 10 psi) for 30 s just prior to use to produce hydrophilic reactive PDMS surfaces.[46,47,57]

Biotin−Streptavidin Patterns. Substrates were incubated with ethanolic solutions of 0.5 mM TEG for ∼17 h to form SAMs. Oxygen plasma-treated PDMS stamps were placed in conformal contact with substrates for 30 min to enable stamp/substrate contact reactions, which caused SAM molecules and underlying Au atoms to be removed from contact areas once stamps were released from the substrates (Figure 1A). Stamps with microscale protruding features (∼30 μm with ∼30−60 μm spacings) or nanoscale protruding or recessed features (200 nm circles with 2 μm pitch or 30 nm lines with 3 μm pitch, respectively) were used for patterning. Post-lift-off substrates were inserted with 80/20 ethanolic solutions of 0.40 mM TEG and 0.1 mM BEG for 1 h. For nanoscale patterning, 100% ethanolic solutions of 0.5 mM BEG were used to maximize BEG insertion into post-lift-off TEG-modified substrates.

Biotinylated substrates were incubated with 10 mg/mL BSA for 5 min to block nonspecific protein adsorption sites, then with 50 μg/mL streptavidin for 20 min, and finally with 100 μg/mL FITC-conjugated rabbit antistreptavidin antibodies for 20 min to visualize streptavidin binding to surface-tethered biotin (Table S1, Supporting Information).

DOI: 10.1021/acs.chemmater.7b01970
Chem. Mater. XXXX, XXX, XXX−XXX

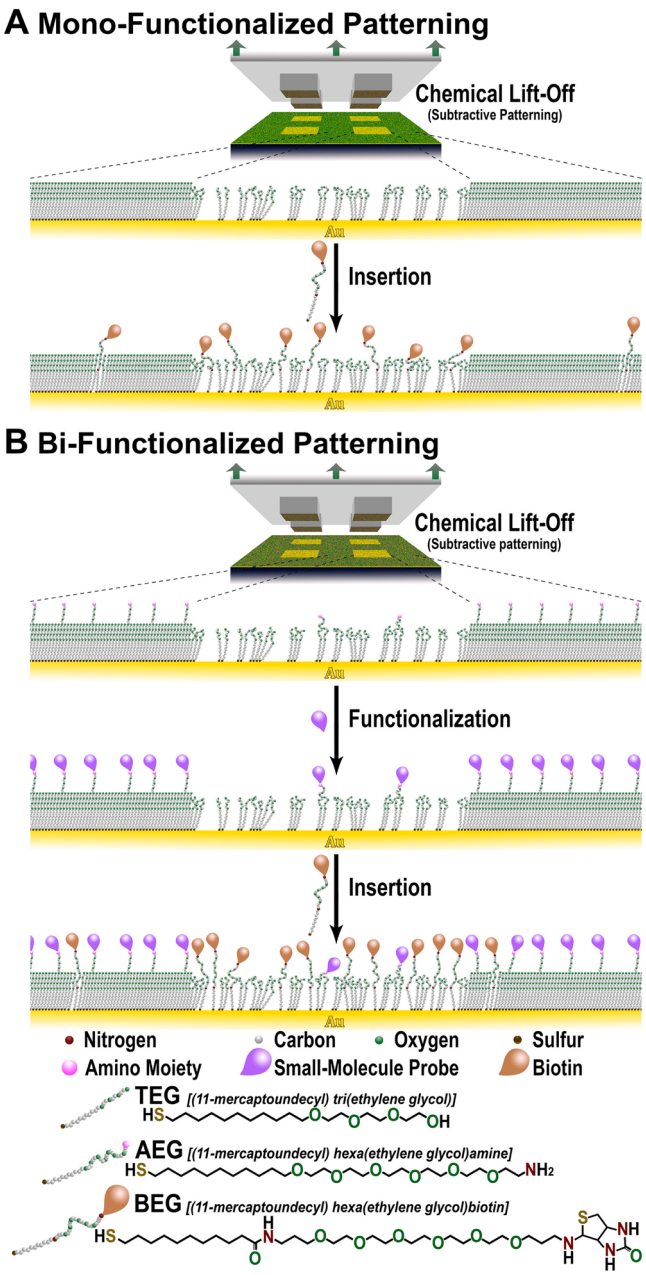

Figure 1. Schematic (not to scale) illustrating single and double patterning *via* chemical lift-off lithography. Preformed SAMs of either (A) hydroxyl-terminated tri(ethylene glycol)alkanethiol (TEG) or (B) mixed 90/10 TEG/amine-terminated hexa(ethylene glycol)alkanethiol (AEG) on Au substrates were chemically lifted off. In part A, substrates were inserted with biotin-terminated hexa(ethylene glycol)-alkanethiols (BEGs). In part B, substrates were first functionalized with small-molecule probes, i.e., L-3,4-dihydroxyphenylalanine or L-5-hydroxytryptophan prior to BEG insertion to form side-by-side patterns.

Copious amounts of deionized water were used to rinse substrates gently after each protein incubation step.

An inverted fluorescence microscope (Axio Observer.D1, Carl Zeiss Microscopy, LLC, Thornwood, NY) was used to image substrates. A 38 HE/high-efficiency filter set with excitation and emission wavelengths at 470 ± 20 and 525 ± 25 nm, respectively, was used to image streptavidin−biotin fluorescence patterns. A 43 HE/high-efficiency filter set with excitation and emission wavelengths at 550 ± 25 and 605 ± 70 nm, respectively, was used to visualize antibody binding to L-DOPA or L-5-HTP substrates (*vide infra*). Fluorescence images were collected using 10× or 20× objective lenses for microscale or nanoscale patterns, respectively. Exposure times were 100 ms (or longer as needed) to visualize differences in fluorescence between the patterned features and the surrounding background or between regions patterned with different probes. The same exposure times were used to image all test and control samples for each experiment. Auto-optimized contrast images were also collected to maximize visualization of nonspecific recognition on control substrates (see Supporting Information).

Fluorescence intensities (arbitrary units) were determined using AxioVs40 version 4.7.1.0 software (Carl Zeiss MicroImaging, Inc.). Fluorescence line scans were adjusted to be approximately the same sizes as patterned features. On average, five line scans were acquired per image. Fluorescence intensities for bright versus dark areas were averaged for each line scan and then for each image. For images with more complex patterns, i.e., UCLA/CNSI letter-shaped features, fluorescence intensities were measured in bright versus dark regions using a histogram function. Fluorescence was quantified from at least three different substrates per condition per experiment.

Streptavidin−biotin nanoscale features were investigated via tapping-mode AFM (Dimension 5000, Bruker AXS, Santa Barbara, CA). Topographic AFM images were collected using Si cantilevers with a spring constant of 48 N/m and a resonant frequency of 190 kHz (Veeco Instruments, Santa Barbara, CA). The resulting images were processed with WSxM 4.0 Beta 6.4 software (Nanotec Electronica, Madrid, Spain).[59]

Side-by-Side Patterning. Substrates were incubated with 90/10 ethanolic solutions of 0.45 mM TEG and 0.05 mM AEG tethers for ∼17 h to create dilute amine-terminated SAMs. Stamps were activated with oxygen plasma and brought into conformal contact with SAM-modified substrates for 30 min to generate stamp/SAM interfacial interactions.

For functionalization with the first probe, which takes place primarily in the unpatterned (non-lifted-off) regions (Figure 1B), solutions of 20 mM FMOC-protected L-DOPA or 40 mM FMOC-protected L-5-HTP were combined with 20 mM or 40 mM NHS/EDC, respectively, in 60/40 DMF/deionized water. This step activates the carboxyl groups of L-DOPA or L-5-HTP with NHS esters for subsequent reaction with the amino moieties of AEG SAM molecules to form amide bonds (Scheme 1). Substrates were incubated with activated L-DOPA or L-5-HTP solutions for 4 h. To functionalize the second probe, substrates were then incubated with 90/10 ethanolic solutions of 0.45 mM TEG and 0.05 mM BEG for 1 h to insert BEG primarily into the patterned (lifted-off) regions (Figure 1B).

The FMOC protecting groups on L-DOPA and L-5-HTP prevented intermolecular reactions between these NHS-activated probe molecules. After immobilization on substrates, FMOC protecting groups were removed with 20% 4-methylpiperidine in deionized water for 20 min. After rinsing with deionized water and drying with nitrogen gas, functionalized substrates were incubated with 10 mg/mL BSA for 5 min, and then with mixtures of streptavidin (50 μg/mL) and either mouse monoclonal anti-L-DOPA primary antibodies or mouse monoclonal anti-L-5-HTP primary antibodies for 20 min, and then with mixtures of FITC-conjugated rabbit polyclonal antistreptavidin antibodies (100 μg/mL) and AlexaFluor 546 goat antimouse IgG secondary antibodies (20 μg/mL) for 20 min to visualize multiplexed protein patterns (Table S1). Imaging was carried out as described above.

Patterning for Membrane-Associated Receptor Capture. Dilute amine-terminated SAMs were produced by incubating substrates with 95/5 ethanolic solutions of 0.048 mM TEG and 0.025 mM AEG for ∼17 h. Substrates were brought into conformal contact for 30 min with the hydrophilic reactive surfaces of oxygen plasma-treated PDMS stamps (25 μm × 25 μm square protruding features). Post-lift-off substrates were functionalized with activated L-5-HTP, and deprotection was carried out using the procedures described in the previous section.

After being rinsed with deionized water, substrates were incubated with 10 mg/mL BSA for 5 min to reduce nonspecific protein binding.[38,45] The L-5-HTP-modified substrates were then incubated

DOI: 10.1021/acs.chemmater.7b01970
Chem. Mater. XXXX, XXX, XXX−XXX

Scheme 1. Schematic Illustrating Surface Functionalization Chemistries[a]

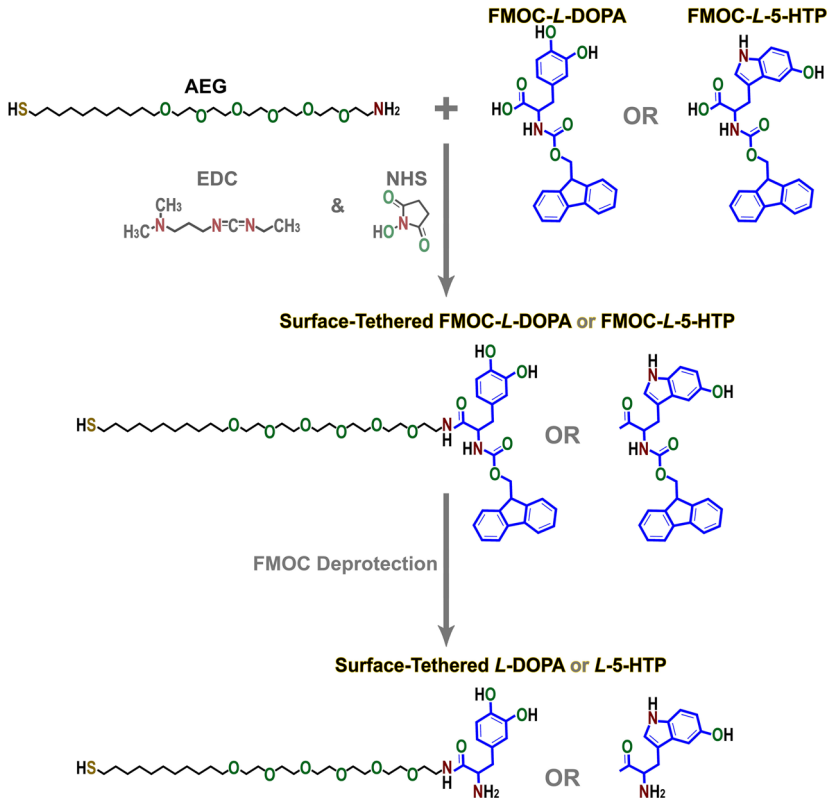

[a]*N*-Hydroxysuccinimide (NHS) and *N*-(3-dimethylaminopropyl)-*N*′-ethylcarbodiimide hydrochloride (EDC) were used to create NHS-ester-activated carboxyl groups on 9-fluorenylmethyloxycarbonyl (FMOC)-protected 3,4-dihydroxy-L-phenylalanine (L-DOPA) or 5-hydroxy-L-tryptophan (L-5-HTP). The NHS esters were then reacted with the amino moieties on amine-terminated hexa(ethylene glycol)alkanethiol (AEG) to form amide bonds. Protecting groups were removed after probe functionalization on substrates to reveal epitopes necessary for recognition by biomolecule partners.

with 100 μg/μL 5-HT$_{1A}$ receptors for 1 h. The receptor-associated cell membranes were not solubilized to retain native receptor conformations favorable for probe recognition.[24,33,38,60] Previously, we found that primary antibodies recognizing membrane-associated receptors have weak affinity for surface-tethered probes.[38] Thus, after incubation with 5-HT$_{1A}$ receptors, functionalized substrates were exposed to antidopamine D$_1$ receptor rabbit polyclonal blocking antibodies for 15 min to reduce nonspecific binding of anti-5-HT$_{1A}$ receptor primary antibodies to surface-tethered L-5-HTP. Substrates were incubated with mouse polyclonal anti-5-HT$_{1A}$ receptor primary antibodies for 15 min followed by 20 μg/mL AlexaFluor 546 goat antimouse secondary antibodies for 15 min to visualize 5-HT$_{1A}$ receptor binding (Table S1). Substrates were rinsed with deionized water between protein incubation steps. The 43 HE fluorescence filter set was used to visualize capture of 5-HT$_{1A}$ receptors to patterns of surface-tethered L-5-HTP as described above.

X-ray Photoelectron Spectroscopy. Featureless PDMS stamps were used for the chemical lift-off process. All XPS data were collected using an AXIS Ultra DLD instrument (Kratos Analytical Inc., Chestnut Ridge, NY). A monochromatic Al Kα X-ray source (10 mA for survey scans and 20 mA for high-resolution scans, 15 kV) with a 200 μm circular spot size and ultrahigh vacuum (10^{-9} Torr) was used.[46,47] Spectra were acquired at a pass energy of 160 eV for survey spectra and 20 eV for high-resolution spectra of Au 4f regions (100 scans) using a 200 ms dwell time.

A charge neutralizer (flood gun) was used to obtain XPS signals on PDMS, which is an insulator. As a result, peaks are shifted slightly from their expected regions. For example, the C 1s peak is 4−5 eV lower than its reference peak at 284.0 eV. Because the number of peaks of interest was small (only Au 4f peaks on PDMS samples), and they were well-separated (~4 eV), peak shifting did not affect peak identification. No corrections were carried out during data collection to shift peaks back to particular regions or to scale peaks based on reference locations.

Statistical Analyses. Data were analyzed by two-tailed unpaired Student's *t*-tests using GraphPad Prism 5.0 (GraphPad Software Inc., San Diego, CA). Fluorescence intensities were normalized to mean values for control regions and are reported as means ± standard errors in relative fluorescence units (RFU) with probabilities $P < 0.05$ considered statistically significant.

■ RESULTS AND DISCUSSION

To explore the flexibility of chemical lift-off lithography as a patterning method for creating functional small-molecule arrays beyond initial findings,[47,48,61] we investigated substrates patterned with the small-molecule biotin (Figure 1A) over a wide variety of feature shapes and sizes (Figure 2). The use of PDMS stamps with different protruding microscale features produced corresponding bright fluorescent patterns (Figure 2A). Relative quantification of the fluorescence in bright versus dark areas of each pattern indicated differential recognition of surface-tethered biotin by streptavidin in the patterned versus unpatterned regions. A lack of measurable fluorescence or patterning was observed when similar substrates were incubated with FITC-labeled antistreptavidin antibodies in the absence of streptavidin indicating negligible nonspecific antibody binding (Figure S1).

A wide-area, bright nanodot array is shown against a dark TEG background in Figure 2B, illustrating a streptavidin−biotin recognition pattern with 100-fold smaller features than in

DOI: 10.1021/acs.chemmater.7b01970
Chem. Mater. XXXX, XXX, XXX−XXX

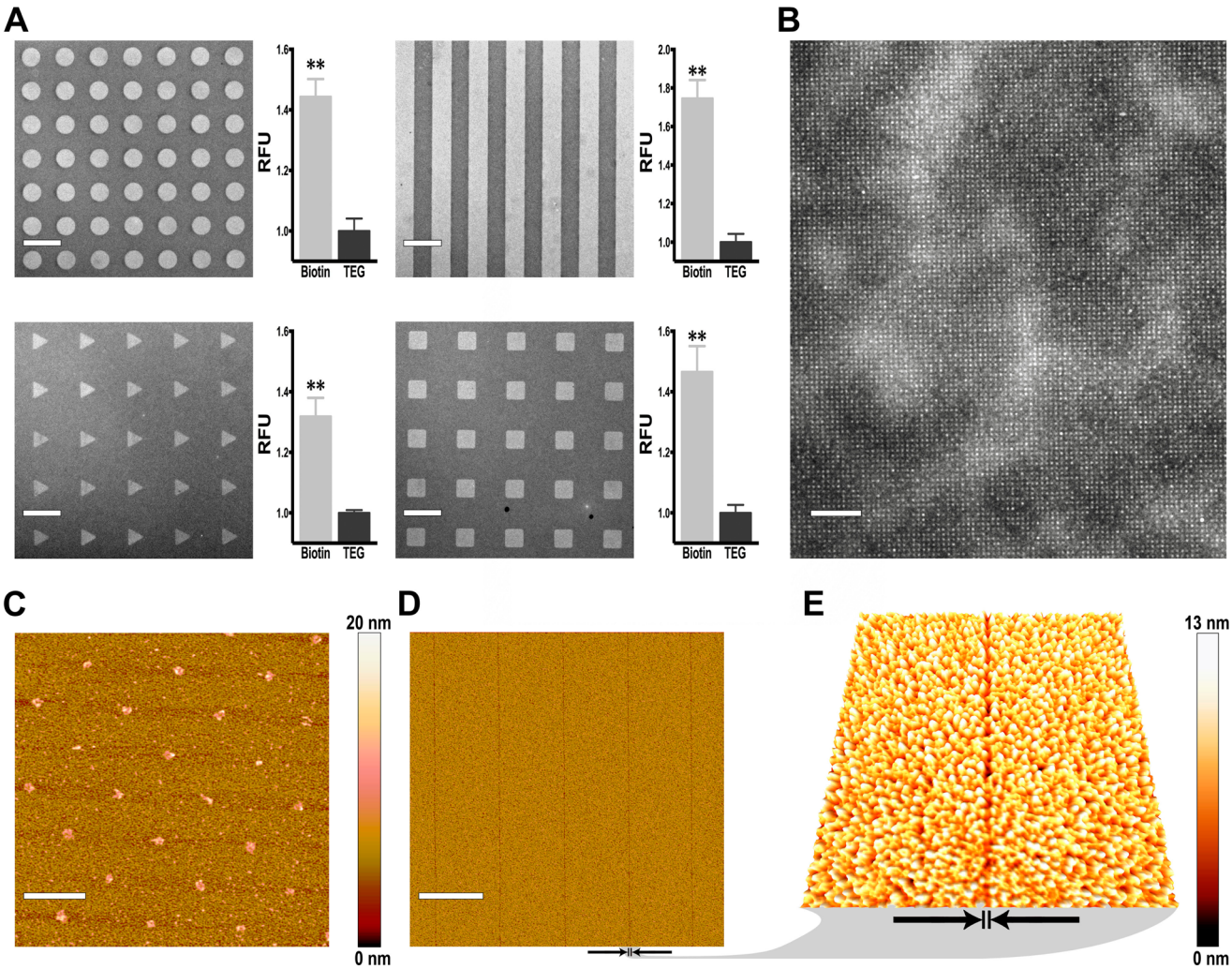

Figure 2. Representative fluorescence and scanning probe images of streptavidin recognition on microscale and nanoscale biotin-patterned substrates. (A) Bright, microscale circular-, striped-, triangular-, or square-patterned regions or (B) nanoscale dots are visualized against a dark surrounding hydroxyl-terminated tri(ethylene glycol)alkanethiol (TEG) background. Binding of streptavidin to surface-tethered biotin was visualized with fluorescein isothiocyanate (FITC)-labeled antistreptavidin antibodies (excitation at 495 nm). Fluorescence images were recorded at an emission wavelength of 519 nm. Error bars represent standard errors of the mean [$N = 3$; $^{**}t < 0.01$ vs unpatterned regions]. (C) Atomic force microscopy (AFM) topography image to quantify sizes of streptavidin−biotin nanodots shown in part B. The dots are 215 ± 3 nm in diameter. In parts D and E, AFM topographic images at two different scales are of sub-30 nm wide TEG lines on a streptavidin−biotin background. The arrows help to visualize the locations of single lines. Scale bars are 60, 40, 2, and 3 μm for A, B, C, and D, respectively. The imaged area is 2 μm × 2 μm in part E.

Figure 2A. Nanodot feature sizes measured by tapping-mode AFM were 215 ± 3 nm in diameter (Figure 2C). Because AFM images were collected under dry conditions, some of the proteins captured on biotin-functionalized dots may have been denatured and/or desorbed contributing to the irregular shapes in Figure 2C.[62]

Previously, we used chemical lift-off lithography to produce features as small as 40 nm using a single lift-off step; double lift-off lithography was needed to pattern 20 nm features.[47] Here, we achieved sub-30 nm feature resolution with single-step lift-off via an inverse patterning strategy; i.e., ultrasmall features were produced in the noncontact areas. Creating nanoscale features in contact areas by conventional additive patterning approaches, e.g., microcontact printing,[63] microdisplacement printing,[64,65] microcontact insertion printing,[66,67] as well as subtractive chemical lift-off lithography, is difficult because protruding, ultrasmall features on PDMS stamps are not mechanically stable during stamp/substrate conformal contact. However, smaller features can be created by deliberately manipulating/distorting stamps.[48,61,68] Employing "hard" PDMS or composite stamp materials and/or hierarchically structured stamps may also enable ultrasmall features in contact regions.[61,69,70]

Tapping-mode AFM was needed to visualize the nanoscale patterns in Figure 2D,E. As shown in Figure 2D, wide lines (∼3 μm) with positive-height topographic features produced by streptavidin recognition of biotinylated (contact) regions are contrasted against narrow TEG features with negative-height topography. Negative features were 26 ± 1 nm wide by AFM (Figure 2E). Since narrow line widths are similar to Au grain sizes on 100 nm polycrystalline Au films (∼20−50 nm), Au graininess increases line-edge roughness and reduces the accuracy of feature size and/or measurement.[71,72] This result suggests further possibilities of using chemical lift-off lithography to produce sub-20 nm or even sub-10 nm features via ultraflat Au films on mica substrates.[73−75]

DOI: 10.1021/acs.chemmater.7b01970
Chem. Mater. XXXX, XXX, XXX−XXX

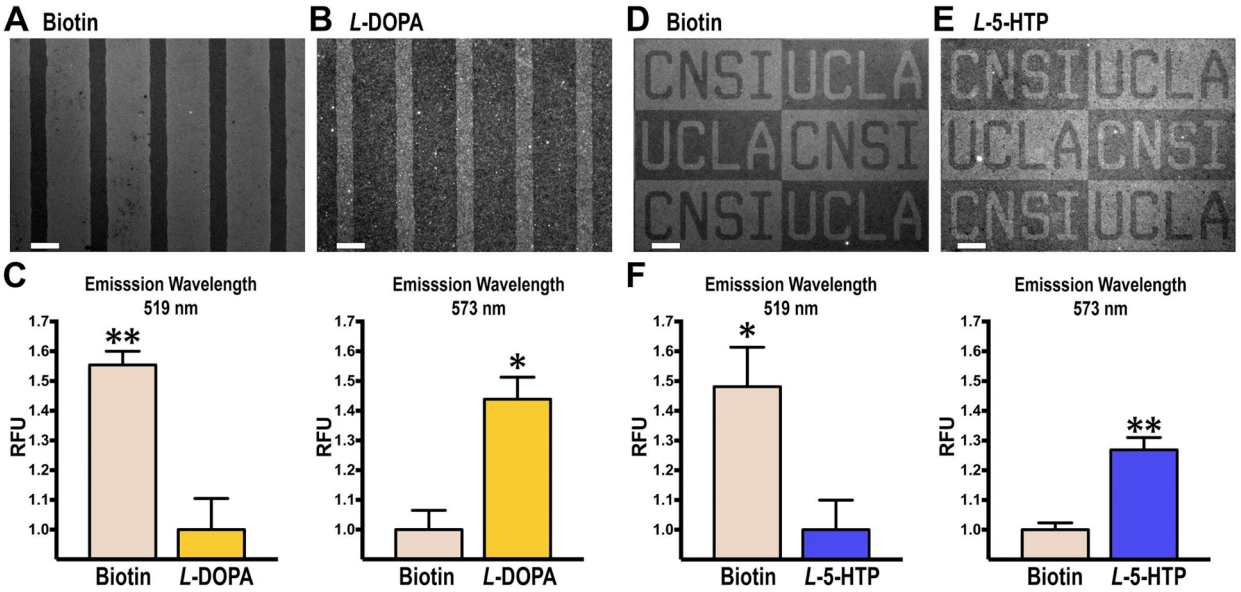

Figure 3. Target sorting on bifunctional substrates. Representative fluorescence images are shown for (A, B) biotin/L-DOPA and (D, E) biotin/L-5-HTP patterned substrates. Substrates were exposed to mixed solutions of streptavidin and anti-L-DOPA or anti-L-5-HTP primary antibodies followed by mixed fluorescein isothiocyanate (FITC)-conjugated antistreptavidin antibodies (excitation at 495 nm) and AlexaFluor 546 secondary antibodies (excitation at 556 nm). Substrates were then imaged at (A, D) 519 nm or (B, E) 573 nm emission wavelengths. In part C, left, significantly higher relative fluorescence intensities were measured in the wide-striped biotin-modified regions vs the narrow-striped L-DOPA-modified regions [$t(4) = 5$, $^{**}P < 0.01$] at the FITC emission wavelength, while in part C, right, significantly higher relative fluorescence intensities were detected in the L-DOPA-modified narrow-striped regions vs the wide-striped biotin-functionalized regions [$t(6) = 3$, $^{*}P < 0.05$] at the AlexaFluor 546 emission wavelength. Similarly, in part F, left, at the FITC emission wavelength, higher relative fluorescence intensities were observed within the UCLA letters and regions surrounding the CNSI letters [$t(4) = 4$, $^{*}P < 0.05$], which were biotin-modified vs surrounding the UCLA letters and within the CNSI letters, which were L-5-HTP-modified regions. In part F, right, opposite fluorescent intensity patterns were quantified at the AlexaFluor 546 emission wavelength [$t(6) = 6$, $^{**}P < 0.01$]. $N = 3-4$ substrates per group. Scale bars are 50 μm.

Above and in previous work, lift-off lithography was used to remove TEG or other hydroxyl-terminated undecanethiol SAM molecules.[47] Here, we extended the use of lift-off lithography to mixed TEG/AEG SAMs. To determine whether stamp contact removes AEG, we used flat PDMS stamps to carry out lift-off on 100% AEG SAMs. Post-lift-off PDMS stamps in contact with AEG-modified Au substrates showed Au 4f XPS signals (Figure S2A), indicating that AEG molecules are liftable.

The AEG in the noncontact regions, as well as any remaining AEG in the contact regions, was functionalized with 3,4-dihydroxy-L-phenylalanine (L-DOPA) or 5-hydroxy-L-tryptophan (L-5-HTP) (Scheme 1). Afterward, insertion of 90/10 TEG/BEG into the contact regions was carried out to create side-by-side biotin/L-DOPA or biotin/L-5-HTP bifunctional patterns (Figure 1B). The BEG and AEG molecules were in low abundance compared to TEG to ensure dilution of surface-tethered biotin and L-DOPA or L-5-HTP[33,38] in the TEG background matrix for efficient capture of large biomolecule binding partners.[76−78] Moreover, low abundance of functional molecules, i.e., AEG in the original SAM or BEG in the insertion solution, minimized residual cross-contamination of side-by-side patterns.

Bifunctionalized substrates were exposed to solutions containing pairs of binding partners, i.e., biotin and anti-L-DOPA or anti-L-5-HTP primary antibodies, to investigate site-specific sorting of biomolecules. Substrates were then exposed to solutions containing FITC-conjugated antistreptavidin antibodies and AlexaFluor 546 secondary antibodies for sorting and visualization of bound streptavidin or primary L-DOPA or L-5-HTP antibodies, respectively.

In Figure 3A, at the fluorescence emission wavelength for FITC-conjugated antistreptavidin antibodies (519 nm), bright wide channels (~75 μm) illustrate streptavidin−biotin recognition in stamp-contact regions. In contrast, dark narrow channels (~30 μm) occur where L-DOPA was functionalized in the noncontact areas. Conversely, in Figure 3B, at the fluorescence emission wavelength for AlexaFluor 546 secondary antibodies (573 nm), bright narrow channels represent anti-L-DOPA antibody recognition of surface-functionalized L-DOPA against dark wide channels where biotin-captured streptavidin occurred.

Similarly, juxtaposed biotin−streptavidin and L-5-HTP/anti-L-5-HTP antibody patterns are shown in Figure 3D,E, respectively, corresponding to fluorescence wavelengths of FITC-conjugated antistreptavidin antibodies (519 nm) and AlexaFluor 546 secondary antibodies (573 nm), respectively. Bright "UCLA" letters and bright regions surrounding the "CNSI" letters in Figure 3D indicate biotin−streptavidin recognition. The "CNSI" letters and bright areas surrounding the "UCLA" letters in Figure 3E indicate L-5-HTP/anti-L-5HTP-antibody binding on the same substrates shown in Figure 3D. Low levels or lack of fluorescence occurred when substrates were incubated with solutions containing FITC-conjugated antistreptavidin antibodies or AlexaFluor 546 secondary antibodies, respectively, without prior exposure to streptavidin and L-DOPA or L-5-HTP primary antibodies (Figure S3). These findings indicate negligible nonspecific binding of the fluorescently labeled antibodies to bifunctional substrates. Importantly, these results demonstrate that bifunctional patterns produced using chemical lift-off lithography could be used to direct capture of neurotransmitter-related

DOI: 10.1021/acs.chemmater.7b01970
Chem. Mater. XXXX, XXX, XXX−XXX

biomolecules including receptors (see below), transporters, and artificial receptors.[6,7,30,33,38]

Variations in intermolecular interactions in mixed versus monocomponent monolayers may impact lift-off yields. Nonetheless, we estimate that lift-off removes ∼70% of AEG molecules (similar to the lift-off yield for TEG molecules). If the mixed monolayers used here nominally contained 5−10% AEG, then ∼1.5−3% of the molecules remaining in the contact regions would be AEG and functionalized with L-DOPA or L-5-HTP. As such, a small amount of anti-L-DOPA or anti-L-5-HTP antibody binding likely occurs in the lift-off regions, which are subsequently functionalized with biotin. Similarly, in mono- and bifunctionalized substrates (Figure 1), small numbers of BEG molecules insert into native SAM defects in the noncontact regions, in addition to insertion in the contact regions. Previously, we used quartz crystal microbalance gravimetry to estimate insertion of alkanethiol molecules similar to BEG into SAM defects in preformed TEG monolayers.[30] We determined that the degree of solution-phase insertion constituted ∼0.5% of the monolayer for 4 h insertion times with 0.2 mM insertion molecules. Here, we inserted BEG into TEG SAMs for 1 h using 0.05−0.1 mM BEG. Thus, the extent of "unintentional" BEG insertion into noncontact region defects is probably <0.5% of the monolayer. Collectively, these effects reduce selective functionalization of contact versus noncontact regions somewhat. However, they appear to have negligible consequences for relative site-specific target recognition under dilute deposition and insertion conditions (Figure 3C,F).

We have shown through the use of small-molecule probes with an additional functional group for linking chemistries that we can retain free functional groups needed for native receptor capture and sorting.[33,46] Earlier patterning was by microcontact insertion printing or microfluidics.[33,38,46] Here, lift-off lithography was used to pattern the small-molecule serotonin precursor L-5-HTP to investigate the capture of native 5-HT_{1A} membrane-associated G-protein-coupled receptors. Because 5-HT_{1A} receptors play critical roles in regulating serotonin neurotransmission in the central nervous system,[79] they are targets for developing treatments for neuropsychiatric disorders.[80,81]

Subtractive patterning was carried out on 95/5 TEG/AEG mixed SAMs. The AEG molecules were then functionalized with L-5-HTP, which has an additional carboxyl moiety compared to serotonin. Anti-5-HT_{1A} receptor primary antibodies and AlexaFluor 546-labeled secondary antibodies were used to visualize L-5-HTP/5-HT_{1A} receptor recognition. Patterns of 5-HT_{1A} receptors appeared in fluorescence microscopy images as bright areas surrounding arrays of dark TEG squares (Figure 4A). Relative fluorescence intensities in L-5-HTP-functionalized (noncontact) regions were significantly greater than in control (contact) regions (Figure 4B). Additional experiments were carried out where similarly patterned substrates were exposed to membranes from cells that do not express 5-HT_{1A} receptors. Substrates were incubated with anti-5-HT_{1A} receptor primary antibodies and AlexaFluor 546-labeled secondary antibodies. Fluorescent patterns were not detectable (Figure S4), indicating negligible nonspecific binding of cell-membranes to patterned L-5-HTP.

To expand chemical lift-off lithography to additional alkanethiols that self-assemble on Au substrates, we investigated lift-off chemistries at stamp/SAM interfaces by varying the terminal functional groups of SAM molecules (Chart 1). X-ray photoelectron spectroscopy characterization of post-lift-off

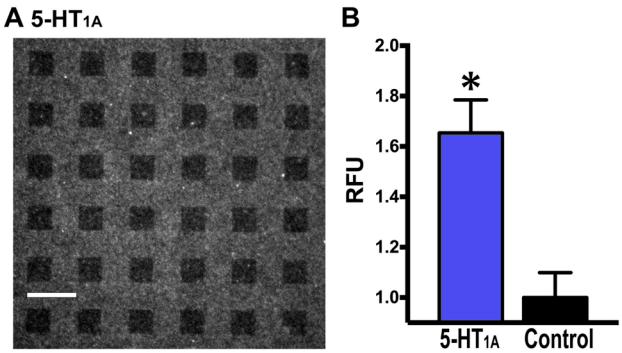

Figure 4. Native receptor capture. (A) Representative fluorescence image of an L-5-HTP-modified substrate exposed to HEK293 membranes from cells overexpressing 5-HT_{1A} receptors, anti-5-HT_{1A} receptor primary antibodies, and AlexaFluor 546 secondary antibodies (excitation at 556 nm). (B) Mean relative fluorescence intensities were significantly different for stamp-noncontact vs contact regions [$t(4) = 4$, $^*P < 0.05$]. Scale bar is 50 μm.

Chart 1. Liftable and Nonliftable Alkanethiols Investigated *via* X-ray Photoelectron Spectroscopy To Detect the Presence/Absence of Au 4f Peaks on Post-Lift-Off Polydimethylsiloxane Stamps[a]

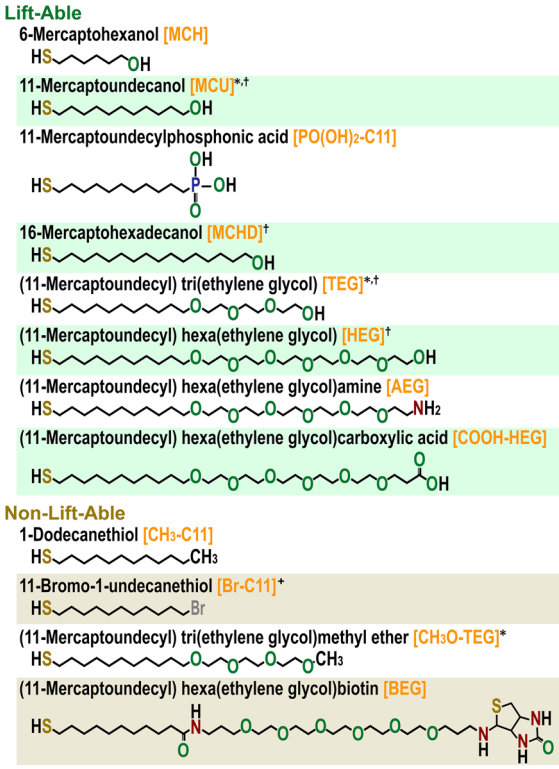

[a]Asterisk refers the reader to ref 47. Dagger refers the reader to ref 56. Plus indicates that the species was investigated by wet chemical etching only.

PDMS stamps (Figure S5) and wet chemical etching (Supporting Information) indicated that, generally, hydrophilic terminal groups, i.e., −OH, −COOH, $-NH_2$, and $-PO(OH)_2$, are amenable to chemical lift-off, presumably because of their abilities to undergo condensation reactions with activated stamp surfaces. By contrast, hydrophobic moieties, i.e., $-CH_3$, $-OCH_3$, and −Br, or the small-molecule probe biotin showed no evidence of lift-off. Chain lengths and SAM ordering may

DOI: 10.1021/acs.chemmater.7b01970
Chem. Mater. XXXX, XXX, XXX−XXX

influence stamp-SAM reactions and lift-off efficiencies; however, XPS does not have the sensitivity to detect potentially subtle differences in lift-off efficiencies.[57] In any case, a shortcoming of lift-off lithography is that not all terminal moieties are amendable to patterning by this method, limiting, to some extent, the on-substrate reactions that can be utilized.

■ CONCLUSIONS AND PROSPECTS

In summary, we broaden the scope of subtractive patterning via chemical lift-off lithography by demonstrating a wide variety of feature shapes and sizes, bifunctional substrates, native protein capture, and a large library of lift-able molecules. Sub-30 nm biopatterning via a single lift-off step was possible using the noncontact areas to advantage. Small-molecule probes were spatially encoded side-by-side on the same substrates to create multiplexed platforms such that targets were directed to the correct probe locations from solution. Small molecules mimicking endogenous neurotransmitters were patterned by lift-off lithography and captured native receptor targets.

One drawback of using chemical lift-off lithography or other stamp-based patterning methods to produce multiplexed substrates involves successive on-substrate probe functionalization steps. Here, we used biotin prefunctionalized molecules, i.e., BEG, to circumvent serial functionalization, which can result in unintended reactions and leaves unreacted surface tethers to contribute to nonspecific target recognition.[82,83] We are investigating the synthesis of a variety of small-molecule prefunctionalized alkanethiols. Preformed 100% TEG SAMs could then be used for lift-off, in place of mixed SAMs, which would obviate tether molecules remaining in the lift-off regions. Post-lift-off substrates could be functionalized via microfluidics to address prefunctionalized molecules to different substrate locations.

Alternately, generating defects by exposing SAM-modified substrates to ultraviolet light or electron irradiation followed by solution deposition of ligand-functionalized molecular substituents could be used to control specific binding of proteins and to generate bifunctional substrates.[84,85] These strategies have been combined with electron-beam lithography to pattern DNA probes on biorepulsive SAMs.[86,87] Although these approaches can be used to create user-defined features, they are limited in terms of sequential processing and time-consuming tuning of ultraviolet wavelength or electron irradiation doses.[84,88,89]

Ongoing efforts to optimize and to understand chemical lift-off lithography mechanistically include collaborative work to characterize and to quantify lift-off and insertion yields further via sum frequency generation spectroscopy.[90] Time-of-flight secondary-ion mass spectrometry (ToF SIMS) may also be useful in this regard. However, charge exchange between neighboring molecules poses challenges, and without detailed information on the ionization efficiencies of each species, quantification, particularly for low-abundance species after lift-off or insertion, is not possible by ToF SIMS.[91] Others and we are investigating the basis of variable reactivities of head groups on different substrates (e.g., −SH on Au vs Ge, or $-PO(OH)_2$ on In_2O_3/SnO_2[92]). We are also determining the unique characteristics of PDMS-supported Au monolayers.[48] In general, multiplexed patterning capabilities, nanoscale biopatterns, as well as the fabrication of thin-film field-effect transistor-based biosensors via chemical lift-off lithography point to the broad applicability of this patterning method.[1,93−95]

■ ASSOCIATED CONTENT

Supporting Information

The Supporting Information is available free of charge on the ACS Publications website at DOI: 10.1021/acs.chemmater.7b01970.

Fluorescence images for experiments investigating nonspecific binding of primary antibodies, secondary antibodies, or cell membranes from untransfected cells to surface-functionalized small-molecule probes; XPS data showing the presence or absence of Au 4f peaks from liftable vs nonliftable alkanethiols, respectively; and table detailing strategies for visualizing biomolecule binding to substrates (PDF)

■ AUTHOR INFORMATION

Corresponding Authors

*E-mail: psw@cnsi.ucla.edu.

*E-mail: aandrews@mednet.ucla.edu.

ORCID

Nako Nakatsuka: 0000-0001-8248-5248

Wei-Ssu Liao: 0000-0002-5619-4997

Andrew C. Serino: 0000-0003-2767-1026

Paul S. Weiss: 0000-0001-5527-6248

Anne M. Andrews: 0000-0002-1961-4833

Author Contributions

The experiments were designed by all authors and carried out by H.H.C., W.-S.L., S.C., and A.C.S. Data were analyzed by H.H.C., N.N., A.C.S., H.Y., and A.M.A. Figures and graphics were designed and prepared by H.Y., N.N., H.H.C., and A.M.A. The manuscript was written by H.H.C., N.N., P.S.W., and A.M.A. with assistance from A.C.S., W.-S.L., S.C., and H.Y. All authors approved the final version of the manuscript and agreed to be accountable for the accuracy and integrity of the work.

Notes

The authors declare no competing financial interest.

■ ACKNOWLEDGMENTS

This work was generously supported by the U.S. Department of Energy (#DE-SC-1037004 for surface patterning and characterization), the National Science Foundation (#CMMI-1636136), the California Neurotechnologies (Cal-BRAIN) Program, and the Kavli Foundation. Prof. Sarawut Cheunkar thanks the government of Thailand for a graduate fellowship. The authors also thank Profs. Steve Baldelli and Nick Winograd, and Drs. Stefanie Altieri, Brian Day, and Jeffrey Schwartz for helpful discussions, and Prof. André Nel, Drs. Ignacio Martini and Liane Slaughter, the Materials Laboratory at the Molecular Instrumentation Center, and the California NanoSystems Institute Nano and Pico Characterization Facility for assistance.

■ REFERENCES

(1) MacBeath, G.; Koehler, A. N.; Schreiber, S. L. Printing Small Molecules as Microarrays and Detecting Protein-Ligand Interactions en Masse. *J. Am. Chem. Soc.* **1999**, *121*, 7967−7968.

(2) LaFratta, C. N.; Walt, D. R. Very High Density Sensing Arrays. *Chem. Rev.* **2008**, *108*, 614−637.

(3) Wittenberg, N. J.; Im, H.; Johnson, T. W.; Xu, X.; Warrington, A. E.; Rodriguez, M.; Oh, S.-H. Facile Assembly of Micro- and Nanoarrays for Sensing with Natural Cell Membranes. *ACS Nano* **2011**, *5*, 7555−7564.

(4) Andrews, A. M.; Weiss, P. S. Nano in the Brain: Nano-Neuroscience. *ACS Nano* **2012**, *6*, 8463−8464.

DOI: 10.1021/acs.chemmater.7b01970
Chem. Mater. XXXX, XXX, XXX−XXX

(5) Tran, H.; Killops, K. L.; Campos, L. M. Advancements and Challenges of Patterning Biomolecules with Sub-50 nm Features. *Soft Matter* **2013**, *9*, 6578−6586.
(6) Alivisatos, A. P.; Andrews, A. M.; Boyden, E. S.; Chun, M.; Church, G. M.; Deisseroth, K.; Donoghue, J. P.; Fraser, S. E.; Lippincott-Schwartz, J.; Looger, L. L.; Masmanidis, S.; McEuen, P. L.; Nurmikko, A. V.; Park, H.; Peterka, D. S.; Reid, C.; Roukes, M. L.; Scherer, A.; Schnitzer, M.; Sejnowski, T. J.; Shepard, K. L.; Tsao, D.; Turrigiano, G.; Weiss, P. S.; Xu, C.; Yuste, R.; Zhuang, X. W. Nanotools for Neuroscience and Brain Activity Mapping. *ACS Nano* **2013**, *7*, 1850−1866.
(7) Andrews, A. M. The BRAIN Initiative: Toward a Chemical Connectome. *ACS Chem. Neurosci.* **2013**, *4*, 645−645.
(8) Tu, S.; Jiang, H. W.; Liu, C. X.; Zhou, S. M.; Tao, S. C. Protein Microarrays for Studies of Drug Mechanisms and Biomarker Discovery in the Era of Systems Biology. *Curr. Pharm. Des.* **2014**, *20*, 49−55.
(9) Andrews, A. M.; Schepartz, A.; Sweedler, J. V.; Weiss, P. S. Chemistry and the BRAIN Initiative. *J. Am. Chem. Soc.* **2014**, *136*, 1−2.
(10) Biteen, J. S.; Blainey, P. C.; Cardon, Z. G.; Chun, M.; Church, G. M.; Dorrestein, P. C.; Fraser, S. E.; Gilbert, J. A.; Jansson, J. K.; Knight, R.; Miller, J. F.; Ozcan, A.; Prather, K. A.; Quake, S. R.; Ruby, E. G.; Silver, P. A.; Taha, S.; van den Engh, G.; Weiss, P. S.; Wong, G. C. L.; Wright, A. T.; Young, T. D. Tools for the Microbiome: Nano and Beyond. *ACS Nano* **2016**, *10*, 6−37.
(11) Nakatsuka, N.; Andrews, A. M. Neurochips Enable Nanoscale Devices for High-Resolution *In Vivo* Neurotransmitter Sensing. *Neuropsychopharmacology* **2016**, *41*, 378−379.
(12) Wassum, K. M.; Ostlund, S. B.; Loewinger, G. C.; Maidment, N. T. Phasic Mesolimbic Dopamine Release Tracks Reward Seeking During Expression of Pavlovian-to-Instrumental Transfer. *Biol. Psychiatry* **2013**, *73*, 747−755.
(13) Yang, H. Y.; Sampson, M. M.; Senturk, D.; Andrews, A. M. Sex- and SERT-Mediated Differences in Stimulated Serotonin Revealed by Fast Microdialysis. *ACS Chem. Neurosci.* **2015**, *6*, 1487−1501.
(14) Wenzel, J. M.; Rauscher, N. A.; Cheer, J. F.; Oleson, E. B. A Role for Phasic Dopamine Release within the Nucleus Accumbens in Encoding Aversion: A Review of the Neurochemical Literature. *ACS Chem. Neurosci.* **2015**, *6*, 16−26.
(15) Wassum, K. M.; Tolosa, V. M.; Tseng, T. C.; Balleine, B. W.; Monbouquette, H. G.; Maidment, N. T. Transient Extracellular Glutamate Events in the Basolateral Amygdala Track Reward-Seeking Actions. *J. Neurosci.* **2012**, *32*, 2734−2746.
(16) Sarter, M.; Lustig, C.; Howe, W. M.; Gritton, H.; Berry, A. S. Deterministic Functions of Cortical Acetylcholine. *Eur. J. Neurosci.* **2014**, *39*, 1912−1920.
(17) Kiyatkin, E. A.; Wakabayashi, K. T. Parsing Glucose Entry into the Brain: Novel Findings Obtained with Enzyme-Based Glucose Biosensors. *ACS Chem. Neurosci.* **2015**, *6*, 108−116.
(18) Andrews, A. M. The Future of Monitoring Molecules. *ACS Chem. Neurosci.* **2015**, *6*, 1−2.
(19) Fang, Y.; Frutos, A. G.; Lahiri, J. Membrane Protein Microarrays. *J. Am. Chem. Soc.* **2002**, *124*, 2394−2395.
(20) Hodneland, C. D.; Lee, Y. S.; Min, D. H.; Mrksich, M. Selective Immobilization of Proteins to Self-Assembled Monolayers Presenting Active Site-Directed Capture Ligands. *Proc. Natl. Acad. Sci. U. S. A.* **2002**, *99*, 5048−5052.
(21) Kwon, Y.; Han, Z.; Karatan, E.; Mrksich, M.; Kay, B. K. Antibody Arrays Prepared by Cutinase-Mediated Immobilization on Self-Assembled Monolayers. *Anal. Chem.* **2004**, *76*, 5713−5720.
(22) Christman, K. L.; Enriquez-Rios, V. D.; Maynard, H. D. Nanopatterning Proteins and Peptides. *Soft Matter* **2006**, *2*, 928−939.
(23) Wong, L. S.; Khan, F.; Micklefield, J. Selective Covalent Protein Immobilization: Strategies and Applications. *Chem. Rev.* **2009**, *109*, 4025−4053.
(24) Fruh, V.; Ijzerman, A. P.; Siegal, G. How to Catch a Membrane Protein in Action: A Review of Functional Membrane Protein Immobilization Strategies and Their Applications. *Chem. Rev.* **2011**, *111*, 640−656.
(25) Nehilla, B. J.; Popat, K. C.; Vu, T. Q.; Chowdhury, S.; Standaert, R. F.; Pepperberg, D. R.; Desai, T. A. Neurotransmitter Analog Tethered to a Silicon Platform for Neuro-BioMEMS Applications. *Biotechnol. Bioeng.* **2004**, *87*, 669−674.
(26) Smith, R. K.; Lewis, P. A.; Weiss, P. S. Patterning Self-Assembled Monolayers. *Prog. Surf. Sci.* **2004**, *75*, 1−68.
(27) Love, J. C.; Estroff, L. A.; Kriebel, J. K.; Nuzzo, R. G.; Whitesides, G. M. Self-Assembled Monolayers of Thiolates on Metals as a Form of Nanotechnology. *Chem. Rev.* **2005**, *105*, 1103−1169.
(28) Vu, T. Q.; Chowdhury, S.; Muni, N. J.; Qian, H. H.; Standaert, R. F.; Pepperberg, D. R. Activation of Membrane Receptors by a Neurotransmitter Conjugate Designed for Surface Attachment. *Biomaterials* **2005**, *26*, 1895−1903.
(29) Gussin, H. A.; Tomlinson, I. D.; Little, D. M.; Warnement, M. R.; Qian, H. H.; Rosenthal, S. J.; Pepperberg, D. R. Binding of Muscimol-Conjugated Quantum Dots to $GABA_C$ Receptors. *J. Am. Chem. Soc.* **2006**, *128*, 15701−15713.
(30) Shuster, M. J.; Vaish, A.; Szapacs, M. E.; Anderson, M. E.; Weiss, P. S.; Andrews, A. M. Biospecific Recognition of Tethered Small Molecules Diluted in Self-Assembled Monolayers. *Adv. Mater.* **2008**, *20*, 164−167.
(31) Wendeln, C.; Singh, I.; Rinnen, S.; Schulz, C.; Arlinghaus, H. F.; Burley, G. A.; Ravoo, B. J. Orthogonal, Metal-Free Surface Modification by Strain-Promoted Azide-Alkyne and Nitrile Oxide-Alkene/Alkyne Cycloadditions. *Chem. Sci.* **2012**, *3*, 2479−2484.
(32) Claridge, S. A.; Liao, W.-S.; Thomas, J. C.; Zhao, Y.; Cao, H. H.; Cheunkar, S.; Serino, A. C.; Andrews, A. M.; Weiss, P. S. From the Bottom Up: Dimensional Control and Characterization in Molecular Monolayers. *Chem. Soc. Rev.* **2013**, *42*, 2725−2745.
(33) Vaish, A.; Shuster, M. J.; Cheunkar, S.; Singh, Y. S.; Weiss, P. S.; Andrews, A. M. Native Serotonin Membrane Receptors Recognize 5-Hydroxytryptophan-Functionalized Substrates: Enabling Small-Molecule Recognition. *ACS Chem. Neurosci.* **2010**, *1*, 495−504.
(34) Claridge, S. A.; Schwartz, J. J.; Weiss, P. S. Electrons, Photons, and Force: Quantitative Single-Molecule Measurements from Physics to Biology. *ACS Nano* **2011**, *5*, 693−729.
(35) Ganesan, R.; Kratz, K.; Lendlein, A. Multicomponent Protein Patterning of Material Surfaces. *J. Mater. Chem.* **2010**, *20*, 7322−7331.
(36) Wendeln, C.; Rinnen, S.; Schulz, C.; Kaufmann, T.; Arlinghaus, H. F.; Ravoo, B. J. Rapid Preparation of Multifunctional Surfaces for Orthogonal Ligation by Microcontact Chemistry. *Chem. - Eur. J.* **2012**, *18*, 5880−5888.
(37) Wendeln, C.; Ravoo, B. J. Surface Patterning by Microcontact Chemistry. *Langmuir* **2012**, *28*, 5527−5538.
(38) Liao, W.-S.; Cao, H. H.; Cheunkar, S.; Shuster, M. J.; Altieri, S. C.; Weiss, P. S.; Andrews, A. M. Small-Molecule Arrays for Sorting G-Protein-Coupled Receptors. *J. Phys. Chem. C* **2013**, *117*, 22362−22368.
(39) Bachas, L. G.; Meyerhoff, M. E. Theoretical-Models for Predicting the Effect of Bridging Group Recognition and Conjugate Substitution on Hapten Enzyme-Immunoassay Dose-Response Curves. *Anal. Biochem.* **1986**, *156*, 223−238.
(40) Ishikawa, E.; Hashida, S.; Kohno, T. Development of Ultrasensitive Enzyme-Immunoassay Reviewed with Emphasis on Factors Which Limit the Sensitivity. *Mol. Cell. Probes* **1991**, *5*, 81−95.
(41) Mrksich, M. Mass Spectrometry of Self-Assembled Monolayers: A New Tool for Molecular Surface Science. *ACS Nano* **2008**, *2*, 7−18.
(42) Mrksich, M. Using Self-Assembled Monolayers to Model the Extracellular Matrix. *Acta Biomater.* **2009**, *5*, 832−841.
(43) Sanchez-Cortes, J.; Bahr, K.; Mrksich, M. Cell Adhesion to Unnatural Ligands Mediated by a Bifunctional Protein. *J. Am. Chem. Soc.* **2010**, *132*, 9733−9737.
(44) Mullen, T. J.; Srinivasan, C.; Hohman, J. N.; Gillmor, S. D.; Shuster, M. J.; Horn, M. W.; Andrews, A. M.; Weiss, P. S. Microcontact Insertion Printing. *Appl. Phys. Lett.* **2007**, *90*, 063114.
(45) Shuster, M. J.; Vaish, A.; Cao, H. H.; Guttentag, A. I.; McManigle, J. E.; Gibb, A. L.; Martinez, M. M.; Nezarati, R. M.; Hinds, J. M.; Liao, W.-S.; Weiss, P. S.; Andrews, A. M. Patterning Small-

DOI: 10.1021/acs.chemmater.7b01970
Chem. Mater. XXXX, XXX, XXX−XXX

Molecule Biocapture Surfaces: Microcontact Insertion Printing vs. Photolithography. *Chem. Commun.* **2011**, *47*, 10641−10643.

(46) Vaish, A.; Shuster, M. J.; Cheunkar, S.; Weiss, P. S.; Andrews, A. M. Tuning Stamp Surface Energy for Soft Lithography of Polar Molecules to Fabricate Bioactive Small-Molecule Microarrays. *Small* **2011**, *7*, 1471−1479.

(47) Liao, W.-S.; Cheunkar, S.; Cao, H. H.; Bednar, H. R.; Weiss, P. S.; Andrews, A. M. Subtractive Patterning *via* Chemical Lift-Off Lithography. *Science* **2012**, *337*, 1517−1521.

(48) Andrews, A. M.; Liao, W.-S.; Weiss, P. S. Double-Sided Opportunities Using Chemical Lift-Off Lithography. *Acc. Chem. Res.* **2016**, *49*, 1449−1457.

(49) Stranick, S. J.; Parikh, A. N.; Allara, D. L.; Weiss, P. S. A New Mechanism for Surface-Diffusion - Motion of a Substrate-Adsorbate Complex. *J. Phys. Chem.* **1994**, *98*, 11136−11142.

(50) Yu, M.; Bovet, N.; Satterley, C. J.; Bengio, S.; Lovelock, K. R. J.; Milligan, P. K.; Jones, R. G.; Woodruff, D. P.; Dhanak, V. True Nature of an Archetypal Self-Assembly System: Mobile Au-Thiolate Species on Au(111). *Phys. Rev. Lett.* **2006**, *97*, 166102.

(51) Moore, A. M.; Mantooth, B. A.; Donhauser, Z. J.; Yao, Y. X.; Tour, J. M.; Weiss, P. S. Real-Time Measurements of Conductance Switching and Motion of Single Oligo(Phenylene Ethynylene) Molecules. *J. Am. Chem. Soc.* **2007**, *129*, 10352−10353.

(52) Han, P.; Kurland, A. R.; Giordano, A. N.; Nanayakkara, S. U.; Blake, M. M.; Pochas, C. M.; Weiss, P. S. Heads and Tails: Simultaneous Exposed and Buried Interface Imaging of Monolayers. *ACS Nano* **2009**, *3*, 3115−3121.

(53) Woodruff, D. P. The Interface Structure of n-Alkylthiolate Self-Assembled Monolayers on Coinage Metal Surfaces. *Phys. Chem. Chem. Phys.* **2008**, *10*, 7211−7221.

(54) Maksymovych, P.; Voznyy, O.; Dougherty, D. B.; Sorescu, D. C.; Yates, J. T. Gold Adatom as a Key Structural Component in Self-Assembled Monolayers of Organosulfur Molecules on Au(111). *Prog. Surf. Sci.* **2010**, *85*, 206−240.

(55) Hakkinen, H. The Gold-Sulfur Interface at the Nanoscale. *Nat. Chem.* **2012**, *4*, 443−455.

(56) Xue, Y. R.; Li, X.; Li, H. B.; Zhang, W. K. Quantifying Thiol-Gold Interactions towards the Efficient Strength Control. *Nat. Commun.* **2014**, *5*, 1−9.

(57) Cao, H. H.; Nakatsuka, N.; Serino, A. C.; Liao, W.-S.; Cheunkar, S.; Yang, H.; Weiss, P. S.; Andrews, A. M. Controlled DNA Patterning by Chemical Lift-Off Lithography: Matrix Matters. *ACS Nano* **2015**, *9*, 11439−11454.

(58) Kim, J.; Rim, Y. S.; Chen, H. J.; Cao, H. H.; Nakatsuka, N.; Hinton, H. L.; Zhao, C. Z.; Andrews, A. M.; Yang, Y.; Weiss, P. S. Fabrication of High-Performance Ultrathin In_2O_3 Film Field-Effect Transistors and Biosensors Using Chemical Lift-Off Lithography. *ACS Nano* **2015**, *9*, 4572−4582.

(59) Horcas, I.; Fernández, R.; Gómez-Rodríguez, J. M.; Colchero, J.; Gómez-Herrero, J.; Baro, A. M. WSXM: A Software for Scanning Probe Microscopy and a Tool for Nanotechnology. *Rev. Sci. Instrum.* **2007**, *78*, 013705.

(60) Hong, Y. L.; Webb, B. L.; Su, H.; Mozdy, E. J.; Fang, Y.; Wu, Q.; Liu, L.; Beck, J.; Ferrie, A. M.; Raghavan, S.; Mauro, J.; Carre, A.; Mueller, D.; Lai, F.; Rasnow, B.; Johnson, M.; Min, H. S.; Salon, J.; Lahiri, J. Functional GPCR Microarrays. *J. Am. Chem. Soc.* **2005**, *127*, 15350−15351.

(61) Xu, X.; Yang, Q.; Cheung, K. M.; Zhao, C.; Wattanatorn, N.; Belling, J. N.; Abendroth, J. M.; Slaughter, L. S.; Mirkin, C. A.; Andrews, A. M.; Weiss, P. S. Polymer-Pen Chemical Lift-Off Lithography. *Nano Lett.* **2017**, *17*, 3302.

(62) Xia, N.; Shumaker-Parry, J. S.; Zareie, M. H.; Campbell, C. T.; Castner, D. G. A Streptavidin Linker Layer That Functions after Drying. *Langmuir* **2004**, *20*, 3710−3716.

(63) Wilbur, J. L.; Kumar, A.; Biebuyck, H. A.; Kim, E.; Whitesides, G. M. Microcontact Printing of Self-Assembled Monolayers: Applications in Microfabrication. *Nanotechnology* **1996**, *7*, 452−457.

(64) Dameron, A. A.; Hampton, J. R.; Smith, R. K.; Mullen, T. J.; Gillmor, S. D.; Weiss, P. S. Microdisplacement Printing. *Nano Lett.* **2005**, *5*, 1834−1837.

(65) Dameron, A. A.; Hampton, J. R.; Gillmor, S. D.; Hohman, J. N.; Weiss, P. S. Enhanced Molecular Patterning *via* Microdisplacement Printing. *J. Vac. Sci. Technol., B: Microelectron. Process. Phenom.* **2005**, *23*, 2929−2932.

(66) Shuster, M. J.; Vaish, A.; Cao, H. H.; Guttentag, A. I.; McManigle, J. E.; Gibb, A. L.; Martinez, M. M.; Nezarati, R. M.; Hinds, J. M.; Liao, W.-S.; Weiss, P. S.; Andrews, A. M. Patterning Small-Molecule Biocapture Surfaces: Microcontact Insertion Printing *vs.* Photolithography. *Chem. Commun.* **2011**, *47*, 10641−10643.

(67) Mullen, T. J.; Srinivasan, C.; Hohman, J. N.; Gillmor, S. D.; Shuster, M. J.; Horn, M. W.; Andrews, A. M.; Weiss, P. S. Microcontact Insertion Printing. *Appl. Phys. Lett.* **2007**, *90*, 063114.

(68) Zhao, C.; Xu, X.; Yang, Q.; Man, T.; Jonas, S. J.; Schwartz, S. J.; Andrews, A. M.; Weiss, P. S. Self-Collapse Lithography. *Nano Lett.* **2017**, DOI: 10.1021/acs.nanolett.7b02269.

(69) Odom, T. W.; Love, J. C.; Wolfe, D. B.; Paul, K. E.; Whitesides, G. M. Improved Pattern Transfer in Soft Lithography Using Composite Stamps. *Langmuir* **2002**, *18*, 5314−5320.

(70) Qin, D.; Xia, Y. N.; Whitesides, G. M. Soft Lithography for Micro- and Nanoscale Patterning. *Nat. Protoc.* **2010**, *5*, 491−502.

(71) Melo, L. L.; Vaz, A. R.; Salvadori, M. C.; Cattani, M. Grain Sizes and Surface Roughness in Platinum and Gold Thin Films. *J. Metastable Nanocryst. Mater.* **2004**, *20−21*, 623−628.

(72) Salvadori, M. C.; Melo, L. L.; Vaz, A. R.; Wiederkehr, R. S.; Teixeira, F. S.; Cattani, M. Platinum and Gold Thin Films Deposited by Filtered Vacuum Arc: Morphological and Crystallographic Grain Sizes. *Surf. Coat. Technol.* **2006**, *200*, 2965−2969.

(73) Diebel, J.; Lowe, H.; Samori, P.; Rabe, J. P. Fabrication of Large-Scale Ultra-Smooth Metal Surfaces by a Replica Technique. *Appl. Phys. A: Mater. Sci. Process.* **2001**, *73*, 273−279.

(74) Ruffino, F.; Torrisi, V.; Marletta, G.; Grimaldi, M. G. Atomic Force Microscopy Investigation of the Kinetic Growth Mechanisms of Sputtered Nanostructured Au Film on Mica: Towards a Nanoscale Morphology Control. *Nanoscale Res. Lett.* **2011**, *6*, 112.

(75) Tan, C.; Cao, X.; Wu, X. J.; He, Q.; Yang, J.; Zhang, X.; Chen, J.; Zhao, W.; Han, S.; Nam, G. H.; Sindoro, M.; Zhang, H. Recent Advances in Ultrathin Two-Dimensional Nanomaterials. *Chem. Rev.* **2017**, *117*, 6225−6331.

(76) Jung, L. S.; Nelson, K. E.; Stayton, P. S.; Campbell, C. T. Binding and Dissociation Kinetics of Wild-Type and Mutant Streptavidins on Mixed Biotin-Containing Alkylthiolate Monolayers. *Langmuir* **2000**, *16*, 9421−9432.

(77) Nelson, K. E.; Gamble, L.; Jung, L. S.; Boeckl, M. S.; Naeemi, E.; Golledge, S. L.; Sasaki, T.; Castner, D. G.; Campbell, C. T.; Stayton, P. S. Surface Characterization of Mixed Self-Assembled Monolayers Designed for Streptavidin Immobilization. *Langmuir* **2001**, *17*, 2807−2816.

(78) Ballav, N.; Terfort, A.; Zharnikov, M. Fabrication of Mixed Self-Assembled Monolayers Designed for Avidin Immobilization by Irradiation Promoted Exchange Reaction. *Langmuir* **2009**, *25*, 9189−9196.

(79) Altieri, S. C.; Garcia-Garcia, A. L.; Leonardo, E. D.; Andrews, A. M. Rethinking 5-HT1A Receptors: Emerging Modes of Inhibitory Feedback of Relevance to Emotion-Related Behavior. *ACS Chem. Neurosci.* **2013**, *4*, 72−83.

(80) Catapano, L. A.; Manji, H. K. G Protein-Coupled Receptors in Major Psychiatric Disorders. *Biochim. Biophys. Acta, Biomembr.* **2007**, *1768*, 976−993.

(81) Richardson-Jones, J. W.; Craige, C. P.; Nguyen, T. H.; Kung, H. F.; Gardier, A. M.; Dranovsky, A.; David, D. J.; Guiard, B. P.; Beck, S. G.; Hen, R.; Leonardo, E. D. Serotonin-1A Autoreceptors Are Necessary and Sufficient for the Normal Formation of Circuits Underlying Innate Anxiety. *J. Neurosci.* **2011**, *31*, 6008−6018.

(82) Sigal, G. B.; Bamdad, C.; Barberis, A.; Strominger, J.; Whitesides, G. M. A Self-Assembled Monolayer for the Binding and

DOI: 10.1021/acs.chemmater.7b01970
Chem. Mater. XXXX, XXX, XXX−XXX

Study of Histidine Tagged Proteins by Surface Plasmon Resonance. *Anal. Chem.* **1996**, *68*, 490−497.

(83) Lahiri, J.; Isaacs, L.; Tien, J.; Whitesides, G. M. A Strategy for the Generation of Surfaces Presenting Ligands for Studies of Binding Based on an Active Ester as a Common Reactive Intermediate: A Surface Plasmon Resonance Study. *Anal. Chem.* **1999**, *71*, 777−790.

(84) Jeyachandran, Y. L.; Terfort, A.; Zharnikov, M. Controlled Modification of Protein-Repelling Self-Assembled Monolayers by Ultraviolet Light: The Effect of the Wavelength. *J. Phys. Chem. C* **2012**, *116*, 9019−9028.

(85) Jeyachandran, Y. L.; Zharnikov, M. Comprehensive Analysis of the Effect of Electron Irradiation on Oligo(Ethylene Glycol) Terminated Self-Assembled Monolayers Applicable for Specific and Nonspecific Patterning of Proteins. *J. Phys. Chem. C* **2012**, *116*, 14950−14959.

(86) Khan, M. N.; Tjong, V.; Chilkoti, A.; Zharnikov, M. Fabrication of ssDNA/Oligo(Ethylene Glycol) Monolayers and Complex Nanostructures by an Irradiation-Promoted Exchange Reaction. *Angew. Chem., Int. Ed.* **2012**, *51*, 10303−10306.

(87) Khan, M. N.; Zharnikov, M. Fabrication of ssDNA/Oligo-(Ethylene Glycol) Monolayers by Promoted Exchange Reaction with Thiol and Disulfide Substituents. *J. Phys. Chem. C* **2014**, *118*, 3093−3101.

(88) Jeyachandran, Y. L.; Weber, T.; Terfort, A.; Zharnikov, M. Application of Long Wavelength Ultraviolet Radiation for Modification and Patterning of Protein-Repelling Monolayers. *J. Phys. Chem. C* **2013**, *117*, 5824−5830.

(89) Jeyachandran, Y. L.; Zharnikov, M. Fabrication of Protein Patterns on the Basis of Short-Chain Protein-Repelling Monolayers. *J. Phys. Chem. C* **2013**, *117*, 2920−2925.

(90) Cimatu, K.; Baldelli, S. Sum Frequency Generation Microscopy of Microcontact-Printed Mixed Self-Assembled Monolayers. *J. Phys. Chem. B* **2006**, *110*, 1807−1813.

(91) Stranick, S. J.; Atre, S. V.; Parikh, A. N.; Wood, M. C.; Allara, D. L.; Winograd, N.; Weiss, P. S. Nanometer-Scale Phase Separation in Mixed Composition Self-Assembled Monolayers. *Nanotechnology* **1996**, *7*, 438−442.

(92) Kim, E.; Park, K.; Hwang, S. Electrochemical Investigation of Chemical Lift-off Lithography on Au and ITO. *Electrochim. Acta* **2017**, *246*, 165−172.

(93) Lueking, A.; Horn, M.; Eickhoff, H.; Bussow, K.; Lehrach, H.; Walter, G. Protein Microarrays for Gene Expression and Antibody Screening. *Anal. Biochem.* **1999**, *270*, 103−111.

(94) Mishina, Y. M.; Wilson, C. J.; Bruett, L.; Smith, J. J.; Stoop-Myer, C.; Jong, S.; Amaral, L. P.; Pedersen, R.; Lyman, S. K.; Myer, V. E.; Kreider, B. L.; Thompson, C. M. Multiplex GPCR Assay in Reverse Transfection Cell Microarrays. *J. Biomol. Screening* **2004**, *9*, 196−207.

(95) Cao, C.; Zhang, J.; Wen, X.; Dodson, S. L.; Dao, N. T.; Wong, L. M.; Wang, S.; Li, S.; Phan, A. T.; Xiong, Q. Metamaterials-Based Label-Free Nanosensor for Conformation and Affinity Biosensing. *ACS Nano* **2013**, *7*, 7583−7591.

DOI: 10.1021/acs.chemmater.7b01970
Chem. Mater. XXXX, XXX, XXX−XXX